Case Study in Mathematical Modelling: Batteries

Zella Baig

HT23

1 Introduction

Batteries are ubiquitous in modern society and demand for them is ever growing, with an expected $\sim 30\%$ increase year on year until 2030 [4]. Naturally, there arise many contexts in which modelling the behaviour of a battery is desirable, such as the usage of electric vehicles where planning a route around charging stations is needed. We seek to construct and implement a model for a battery and apply it to precisely such a scenario, namely seeking an optimal usage profile for an electric vehicle for a given constrained driving problem (that is to say, given a set journey with certain constraints). We hope that the results and insights gathered from this toy model could be readily extended to further applications.

We split our approach into two broad contexts: performance, and degradation. Performance is concerned with how the battery behaves under given conditions, and degradation is concerned with how the battery capacity degrades over time. The justification for such an approach arises from the ideas that

1. Ideally, we want to *use* (or extract utility from) our batteries as much as possible for a given context,

2. All batteries die at some point, which limits how much utility we can extract from them.

With these points in mind, we seek to both construct and apply our models.

2 Preliminaries

2.1 Mathematical Models

There exist two broad approaches to mathematically model battery behaviour: *equivalent circuit models* (ECMs), and *physical models* [13]. Broadly speaking, the former approach seeks to replicate the observed behaviour of batteries with "fictional" idealised circuit parameters, such as an ideal voltage source which might be coupled with a resistor to showcase the (observed) internal resistance of a cell. With a sufficiently complex model as to account for observed battery data for a given scenario, the hope is that ECMs then allow for relatively simple and computationally cheap modelling of batteries without needing to account for any physical behaviour occurring within the cells themselves.

On the other hand, physical models seek to accurately model the electrochemical processes occurring within batteries. Naturally, these give more accurate results as they

allow for a more cohesive view of what effects occur in batteries as opposed to ECMs which only offer simplified parameters that give the expected observations. The key drawback with physical models, however, lies within the complexity of such models. Modelling minute physical changes is necessarily more complex than considering a few discrete idealised circuit parameters, and these costs increase significantly in any context in which we require rapid modelling (such as in on-board computers).

Thus, seeking to implement the simplest and "cheapest" possible model of a battery for our scenario, we seek to utilise an ECM. However, before we do so, we pause to introduce the specific cell that we seek to model. Note that we constrain ourselves to modelling a specific cell with the goal producing as realistic of an analysis as possible, but much of the approach we utilise may be readily extended to other cells.

2.2 Battery Data

The specific cell that we model is a Panasonic 18650PF Lithium-Ion (Li-Ion) battery, a rechargeable cell with a maximum capacity of 2.9 Ah, and maximum rated current of 10 A [8]. This cell was chosen for two primary reasons:

1. Li-Ion cells are an incredibly common type of battery for many purposes (notably electric vehicles) [9].

2. This cell has a comprehensive dataset with Hybrid Pulse Power Characterisation (HPPC) curves, which give values for different parameters of the cell (such as voltage) for a given current (or power) profile [5], and information on capacity degradation over time [8].

The existence of the HPPC curves for this cell is crucial in constructing an appropriate ECM for our battery: if we have information on how the cell actually performs for a given input profile and we have some model which roughly mimics this behaviour, we would then be able to perform a simple optimisation routine on our model to determine what values our circuit parameters take.

The HPPC tests for our cell consist of 20 different pulses of current, performed at increments of 5% *state of charge* (s), which is a dimensionless parameter defined by

$$s(t) = s(t_0) - \int_{t_0}^{t} dt\, \frac{I(t)}{Q(t)}, \tag{1}$$

with $I(t)$ being the elapsed current (with discharging corresponding to a positive current), and $Q(t)$ being the capacity of the cell at time t. Intuitively, $s = 1$ corresponds to a fully charged cell, and $s = 0$ corresponds to a depleted cell.

2.3 Equivalent Circuit Model

We examine the HPPC pulse given in Figure 1. We use the justification that the voltage response for a fixed current strongly resembles that of an RC circuit charge-discharge pulse to then guide the construction of our ECM.

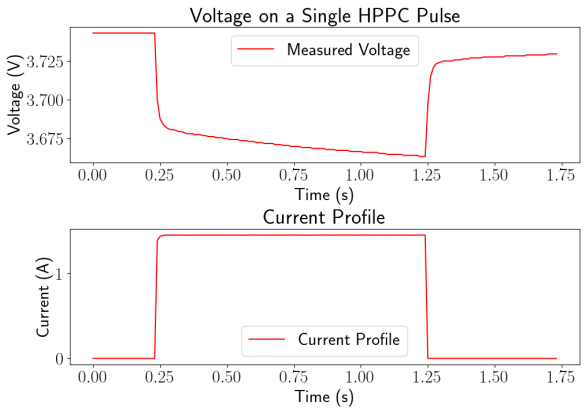

Figure 1: A single current pulse applied to our cell with the corresponding voltage response in time.

Noting also that we observe a voltage drop below the rated voltage of our cell when a given load is attached, we seek to construct an ECM of the form given in Figure 2. Discussing each facet of the model in turn, we have:

- The ideal voltage source V_{OC}, connected in series with the resistor R_0 which denotes the internal resistance of the cell.
- A parallel RC pair $(R_1 C_1)$ connected in series with the internal resistance and open circuit voltage, which provides the appropriate charge-discharge behaviour with a corresponding voltage drop V_1.
- The total current draw $I(t)$ with the relation $I = I_{C_1} + I_{R_1}$ via Kirchhoff's Current Law (KCL).
- The total voltage draw $V(t)$ with the relation $V = V_{OC} - V_0 - V_1$, via Kirchhoff's Voltage Law (KVL).

Further, we readily observe from the HPPC data that there seems to be some dependence on s for our ECM parameters, which can be shown in Figure 3. We can perform a simple curve-fitting procedure to construct polynomials (given in Appendix A) to represent the behaviour of parameter values as functions of $s(t)$.

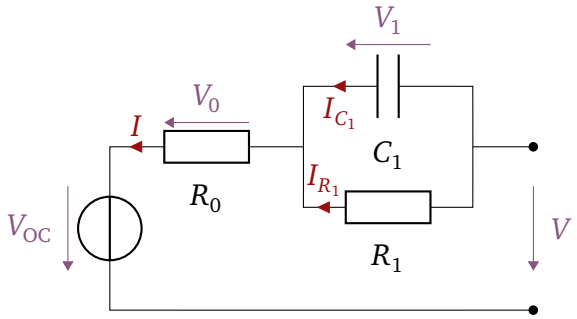

Figure 2: ECM to describe voltage behaviour for a pulsed current.

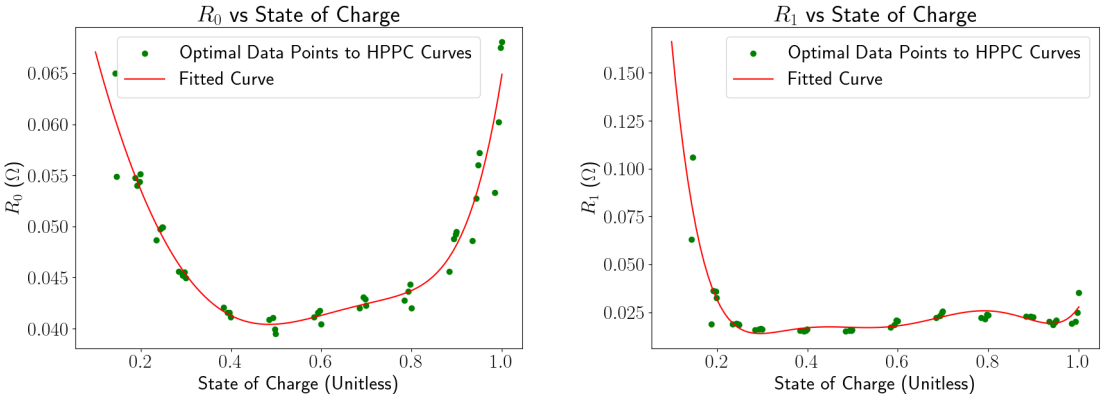

(a) Fit of R_0 as a function of state of charge.

(b) Fit of R_1 as a function of state of charge.

Figure 3: Example fits of ECM parameters as a function of state of charge $s(t)$.

We follow the procedure outlined in [13] to now construct the system of equations for our ECM, and so we first re-express our voltage conservation equation as

$$V(s,t) = V_{OC}(s) - R_1(s)I_{R_1}(t) - R_0(s)I(t). \tag{2}$$

Next, by dropping all explicit dependence on all variables in the arguments and with $\dot{A}$ denoting the rate of change with respect to time, we have

$$\dot{V}_{C_1} = \frac{I_{C_1}}{C_1}, \tag{3}$$

$$V_{C_1} = V_1 = R_1 I_{R_1}, \tag{4}$$

and thus rearranging KCL we have:

$$I_{R_1} + I_{C_1} = I, \tag{5}$$
$$I_{R_1} + C_1 \dot{V}_{C_1} = I, \tag{6}$$
$$C_1 R_1 \dot{I}_{R_1} = I - I_{R_1}, \tag{7}$$
$$\dot{I}_{R_1} = \frac{I}{R_1 C_1} - \frac{I_{R_1}}{R_1 C_1}. \tag{8}$$

Then, using (1), (2), (8), and the relationship $P = IV$ we can construct an initial system of equations to be solved, assuming a constant capacity over time, for battery performance for a given input profile (noting that we re-introduce all variable dependence for clarity):

$$ECM_0 \begin{cases} \dot{s}(t) = -\dfrac{I(t)}{Q} & (9) \\ V(s,t) = V_{OC}(s) - R_1(s) I_{R_1}(s,t) - R_0(s) I(t) & (10) \\ \dot{I}_{R_1}(s,t) = \dfrac{I(t)}{R_1(s) C_1(s)} - \dfrac{I_{R_1}(s,t)}{R_1(s) C_1(s)} & (11) \\ P(t) = I(t) V(s,t) & (12) \end{cases}$$

At this point, the key fault in our model ECM_0 is the assumption that capacity Q remains constant in (9), and so we turn towards developing a model for capacity degradation.

2.4 Capacity Degradation

Literature suggests that we observe two types of degradation effects within batteries [12]:

1. Calendar ageing, which occurs independently of any usage over the span of weeks and months.

2. Cycle ageing, which occurs as a result of drawing current from the battery during usage.

We use the term “cycle” to refer in this context to a discrete variable, with one cycle corresponding to one complete discharge and charge of battery[1] , regardless of the

[1]Note that we can easily extend cycles to be a continuous variable by referring to *fractional* cycles. For example 2.5 cycles would refer to enough current having been drawn from the battery to deplete it and charge it twice over, and then deplete it once again.

time frame of the discharge. The main underpinning of our approach towards capacity degradation is the utilisation of this fact. Namely, knowing that calendar ageing occurs over long time frames and cycle ageing is *very likely* to occur on much shorter time frames (over the span of minutes or hours), we can linearise any expression we have for capacity degradation in these two variables. We thus posit a degradation function of the form

$$\Delta Q(t) = -(\Delta Q)_{cal} - (\Delta Q)_{cycle}\,. \tag{13}$$

2.4.1 Calendar Degradation

Focusing on calendar degradation first, we motivate our degradation through the observation of several behaviours [16]:

- From the battery data sheet we know that we observe a linear capacity degradation with time [11].
- There is an optimal state of charge to store the battery at, at roughly $s \approx 0.4$ [10].
- There exists some sort of penalty effect wherein using an older battery is worse for capacity fade than using a new battery, and that this penalty effect is lessened when within a (cell-dependent) range of s [16].

As such, we postulate that our calendar degradation function behaves as

$$\left(\frac{\partial Q}{\partial t}\right)_{c,s,I} = -m_1 f(s), \tag{14}$$

$$\left(\frac{\partial Q}{\partial s}\right)_{c,t,I} = -m_2 g(s) t, \tag{15}$$

with m_1, m_2 positive constants, and $f(s), g(s)$ some convex non-negative functions with $\min g(s) = 0, \min f(s) = 1$ such that we introduce penalties outside optimal state of charge values with $g(s)$, and steepen the linear decrease with time outside the optimal state of charge value with $f(s)$. Here, (14) represents the of linear decrease of capacity over time with the coefficient m_1 being found from the data sheet (which lists capacity fade at three months, which we extrapolate from), and the function $f(s)$ is chosen to be $f(s) \sim \cosh(s)$, scaled appropriately to give a minimum at $s = 0.4$.

The penalty effect (15) presented slightly more of a challenge wherein we did not have precise data for our battery on how this function behaves. As such, we chose to model this effect with the constraint[2] that $m_2 g(s) = m_1 \left|\frac{df}{ds}\right|$, once again fulfilling the

[2]This constraint is chosen such that we may ultimately write the calendar degradation function in a form resembling an integral of a total derivative.

criteria we desire. To illustrate the effect of this penalty function further, consider Figure 4 which plots $\frac{\partial Q}{\partial s}$ for two different time values, with an "old" battery shown in green, and a "new" battery shown in red.

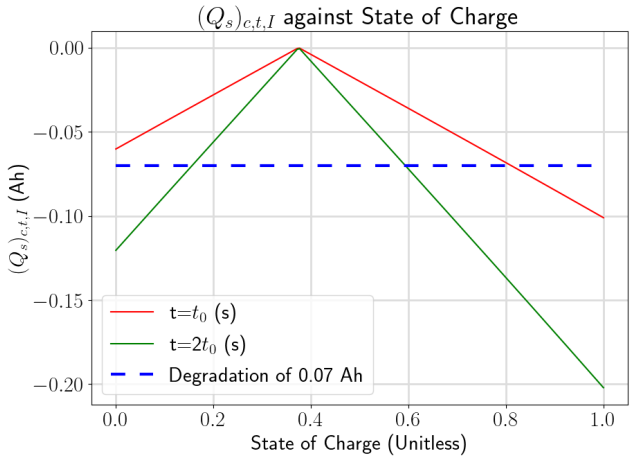

Figure 4: Analysis of calendar ageing "penalty functions" for two different ages of battery.

Assuming we do not wish to go below a certain degradation, shown in the blue dashed line, the range of effective states of charge we can keep the battery at are shown in the regions lying above the blue line; the "new" battery can operate at any state of charge under $s \approx 0.8$, while the "old" battery has a much narrower range of acceptable s values, lying roughly between 0.1 and 0.6. Thus, we can define $(\Delta Q)_{cal}$ as the *calendar ageing factor* F_{cal}

$$(\Delta Q)_{cal} := F_{cal}(t,s) = \int dt \left(\left(\frac{\partial Q}{\partial s} \right)_{c,t,I} \left| \frac{ds}{dt} \right| + \left(\frac{\partial Q}{\partial t} \right)_{c,s,I} \right), \tag{16}$$

where the absolute sign on $\frac{ds}{dt}$ arises from the fact that we seek to model charging as also incurring a degradation cost, and so the rate of change of s may be either positive or negative. We would like to draw attention to the fact that the "penalty effect" term $\left(\frac{\partial Q}{\partial s}\right)$ is multiplied by $\left|\frac{ds}{dt}\right|$ in (16). The effect of this term is such that we only "see" the penalty effect once we *use* the battery, i.e. when the state of charge is changing via current being drawn or inputted. In other words, this effect is unseen if no current is being drawn from the battery, but we expect (as this term is proportional to t) that as $t \to \infty$ for this term to dominate any ageing effects when the battery *is* in use. Having found an expression for calendar degradation, we move now towards discussing cycle degradation of capacity.

2.4.2 Cycle Degradation

It is known that cycle ageing in batteries displays linear behaviour until what is commonly referred to as the *knee point*, at which we see a sharp decrease in capacity with cycles in a highly non-linear fashion [14]. We illustrate this in Figure 5(a), with the manufacturer-provided cycle degradation curve shown in blue [8] (which cuts off at 500 cycles), at which point we draw on an exaggerated knee point in red.

Importantly, this curve is given for a single current: at 1 C, or 2.9 A [3], whereas we wish to ideally describe how cycle ageing occurs at an arbitrary current. In order to begin to do so, we first add artificial points onto the data given in Figure 5(a). We then perform a simple fit to a function of the form

$$F(c) = c\left(\alpha_1 + \alpha_2 \exp\left\{\alpha_3(c-\alpha_4)\right\}\right), \tag{17}$$

with all $\alpha_i \geq 0$. We present the result of this fit in Figure 5(b).

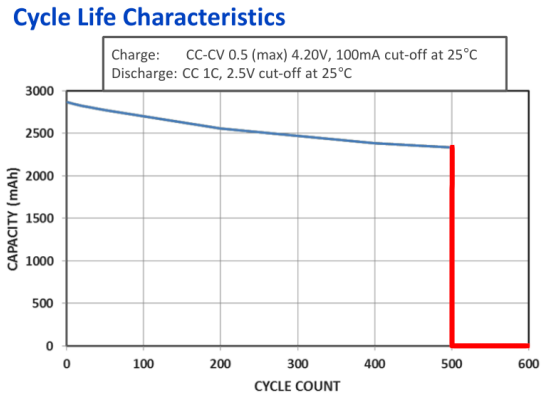

(a) Analysis of manufacturer-provided cycle degradation curve with artificial "knee" behaviour shown in red.

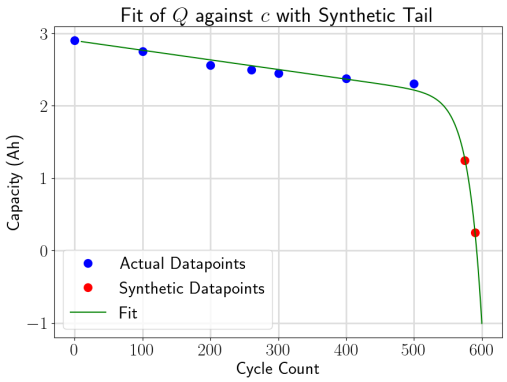

(b) Fit of cycle degradation curve ($Q_0 - F(c)$) with actual and synthetic data points highlighted, with $F(c)$ as defined in (17).

Figure 5: Cycle degradation curves for a current of 2.9A.

We dub the function $F(c)$ the *current agnostic cycle degradation factor*, which we write as $F_{acycle}(c)$.

Seeking now to incorporate current dependence, we incorporate results from [12], in which the authors analyse the current-dependant degradation of a 1.4 Ah Li-Ion battery for current ranges between $1-3$ C, up to a maximum of 300 cycles. Within this paper, the authors describe a fit of degradation of the form

$$Q(c) \approx \beta_1(I)e^{a(I)c} + \beta_2(I)e^{b(I)c}, \tag{18}$$

[3] A current of n C corresponds to nQ_0 A, with Q_0 in Ah.

and we make the simplifying assumption in (18) that β_1, β_2 are constant (justified by the observation that the variation they observe in β_1, β_2 is far smaller than the variations in a, b).

We perform a simple fitting procedure to their data to generate $a(I), b(I)$ for currents in the range[4] 1 C $\leq I \leq$ 3 C; with these we are able to generate an arbitrary capacity degradation as a function of cycle count for currents lying within this range, when using considering the cell in [12]. Subsequently, we generate several different degradations for currents lying in the range 1 C $\leq I \leq$ 3 C, and consider the values at 300 cycles (which, given the nature of the degradation profiles, represent the "maximum" degradation we observe within 300 cycles). Finally, we apply a fit to the degradations in the capacity at 300 cycles at current n C; the justification for doing so is the assumption that while actual current values in amperes that cause a certain amount of degradation might vary significantly between batteries, the current in C should behave roughly similarly from one battery to the next.

This final fit, of the form (with α_i again non-negative)

$$F(I) = \alpha_5 - \exp\left\{\alpha_6 I - \alpha_7\right\}, \tag{19}$$

we dub the *current scaling factor* $F_{current}(I)$. We further further constrain $F_{current}$ to lie in the range $0 \leq F_{current} \leq 1$. $F_{current}$, in essence, is a measure of how much *further* the capacity should be decreased by for a given cycle degradation, dependant on the current at which the battery was cycled. A value of $F_{current} = 1$ would mean that our battery was ran at $I \leq 1C$, and lower values of $F_{current}$ correspond to higher values of current. We present $F_{current}(I)$ in Figure 6.

Clearly, this analysis of $F_{current}(I)$ has taken several liberties in the generation of the factor, but we claim that our results are indeed reasonable given that our combined cycle degradation function,

$$(\Delta Q)_{cycle} := F_{cycle}(I, c) = \frac{F_{acycle}(c)}{F_{current}(I)} \tag{20}$$

blows up to infinity as we approach an operating current of $\approx$ 17 A as shown in Figure 6; this is reasonably correct as the maximum allowable current for this cell as stated on the data sheet to be 10 A. Further, we can see from Figure 6 that we incur heavy degradation for current operation above 10 A, which is again in line with physical results to within a few amperes, suggesting that our cycle degradation function is indeed reasonable.

[4]The behaviour for these variables is highly non-linear and as such for currents outside this range we observe non-physical results with the fit we have.

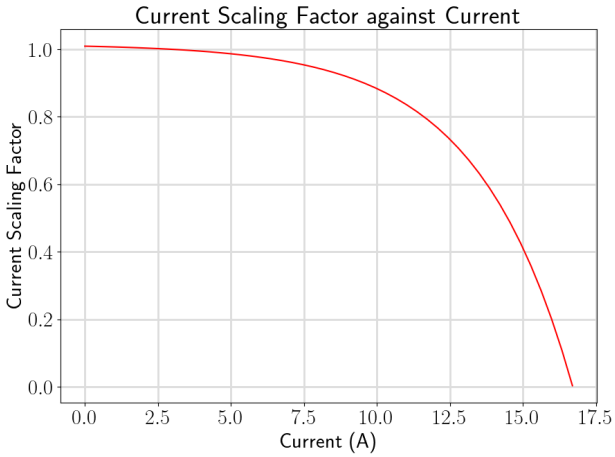

Figure 6: $F_{current}(I)$ for all allowed values of current with the constraint that $0 \leq F_{current} \leq 1$.

Thus, we put together our expressions for cycle and calendar degradation to determine the final expression for capacity:

$$Q(t,c,s,I) = Q_0 - \frac{F_{acycle}(c)}{F_{current}(I)} - F_{cal}(t,s) \tag{21}$$

$$= Q_0 - \frac{c\left(\alpha_1 + \alpha_2 \exp\{\alpha_3 c - \alpha_4\}\right)}{\alpha_5 - \exp\{\alpha_6 I - \alpha_7\}} - \int_0^t dt \left(\alpha_8 \cosh\left(\alpha_9 s - \alpha_{10}\right) + \alpha_{11} t \left|\sinh\left(\alpha_9 s - \alpha_{10}\right)\right| \left|\frac{ds}{dt}\right|\right), \tag{22}$$

with $\alpha_i \geq 0$ and the values given in Appendix B.

We also present our combined degradation effects in Figure 7 (assuming storage at the same state of charge for all profiles as we have already discussed this effect in Figure 4). Note in particular how a longer storage duration incurs a downwards translation of the degradation curve, and a higher current usage causes a steeper gradient in the "linear" part of the degradation curve, and thus an earlier knee point.

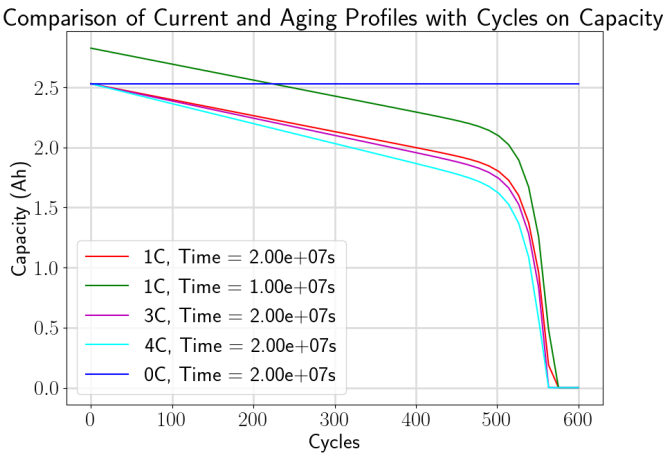

Figure 7: Comparison of degradation profiles for different current usages and ages, all at the same state of charge.

3 Formulation of Problem

Now that we have constructed a model for capacity, we can update ECM_0 (equations 9 – 12) to no longer be constrained with a constant capacity, which we present as

$$ECM_1 \begin{cases} Q(t,c,s,I) = Q_0 - \dfrac{F_{acycle}(c)}{F_{current}(I)} - F_{cal}(t,s) & (23) \\ \dot{s}(t,c,s,I) = -\dfrac{I(t)}{Q(t,c,s,I)} & (24) \\ V(s,t) = V_{OC}(s) - R_1(s)I_{R_1}(s,t) - R_0(s)I(t) & (25) \\ \dot{I}_{R_1}(s,t) = \dfrac{I(t)}{R_1(s)C_1(s)} - \dfrac{I_{R_1}(s,t)}{R_1(s)C_1(s)} & (26) \\ P(t) = I(t)V(s,t), & (27) \end{cases}$$

whilst keeping the expression for capacity in the condensed form (21) for clarity. This system of equations is then capable of being solved numerically, such as via ode15s, a variable order ODE solver in MATLAB [7].

The problem we seek to analyse is seeking an optimal driving routine for a simple graph as presented in Figure 8, where a user spends the week at home but must traverse 115 km on the every weekend to get to another location (such as work), and then go back home again after staying for two days. Further assuming that the electric car battery cannot last the entire distance on a single charge, we insert two charging stations at distances 20 km and 85 km from home. Lastly, we assume that upon every return home

we charge to 0.8 state of charge (a common threshold for electric vehicles [6]).

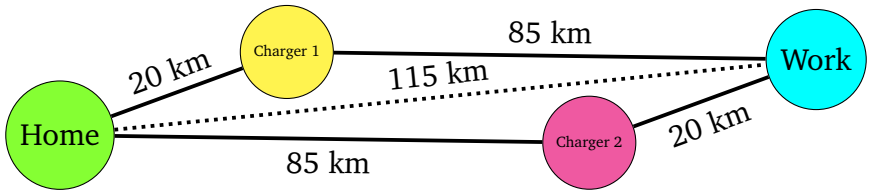

Figure 8: Pictorial representation of optimisation problem, with possible routes shown in solid lines and total distance between work and home shown on the dotted line.

We thus define C_1 as the distance travelled before stopping at a charging station, and then $C_2 := 330 - C_1$ as the distance left for the rest of the weekend trip to return home[5]. We then define all the possible trips, and present them in Table 1. Note that Routes 1 and 4 charge at Charging Station 1, and Routes 2 and 3 stop at Charging Station 2 - meaning that Route 1 and Route 4 have a long leg and a short leg, whilst Route 2 and Route 3 have two "medium" legs of the journey.

Route:	Route 1:	Route 2:	Route 3:	Route 4:
C_1:	20 km	85 km	145 km	210 km
C_2:	210 km	145 km	85 km	20 km

Table 1: Outline of possible routes, with C_1 being the distance travelled until charging at a charging station, and C_2 being the distance left until the user returns home.

4 Results

Defining state of health as the ratio $\frac{Q(t,c,s,I)}{Q_0}$, we build up to our final results by considering each ageing effect in turn. First, we present the results of only considering cycle ageing in Figure 9, where the routes with the long and short leg (Routes 1 and 4) clearly lead to worse degradation over time.

We justify this result in Figure 10, which shows whilst driving (the only time when we need to consider cycle ageing effects) the mean $V_{oc}(s)$ for the routes with a long and short leg is lower. As $V(s,t) \propto V_{oc}(s)$, and $V(s,t) \propto \frac{1}{I(t)}$, we see that Routes 1 and 4 actually lead to a higher current draw assuming a constant power output required for

[5]We make the implicit assumption that we only make one stop during the entire trip to charge, and also note that we drive at a fixed velocity. Further assume we are at a fixed temperature of 10° celcius.

our vehicle. As a higher current implies a smaller value for $F_{current}(I)$, this then leads to a greater degradation over time.

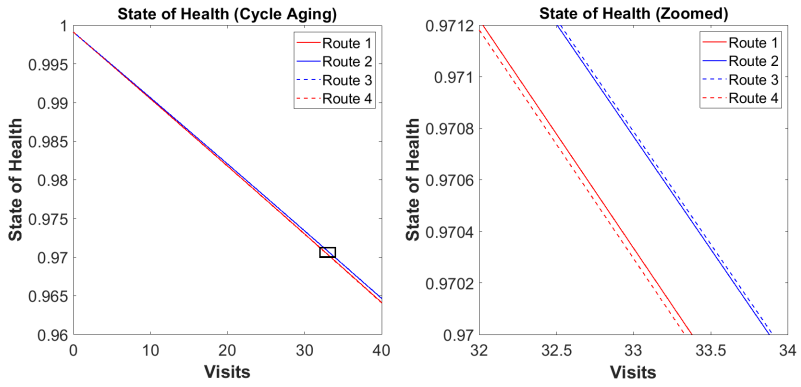

Figure 9: State of health as a function of only cycle ageing effects. Note that a visit is defined as a round trip to work and back.

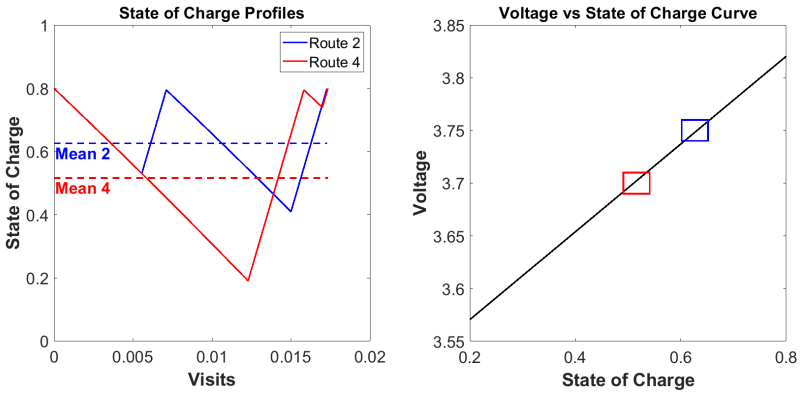

Figure 10: Mean state of charge while driving for Routes 2 and 4, with these state of charge values highlighted on the $V_{oc}(s)$ curve generated from ECM_1.

We next discuss the effect of solely incorporating calendar ageing, which we present in Figure 11. Note how we see two different behaviours: at early times (a "new battery") the routes with the long and short leg perform worse, as when we considered only cycle ageing effects. However, as we increase the number of visits (an "old battery") the two routes with the medium legs begin to perform worse, with the switch happening at around 20 visits.

Then, examining the average state of charge over a visit (including time spent not driving) for new batteries as shown in Figure 12, we see that the routes with two medium legs have an average state of charge that is nearer to the optimal value of 0.4 - meaning that these routes incur less degradation for new batteries.

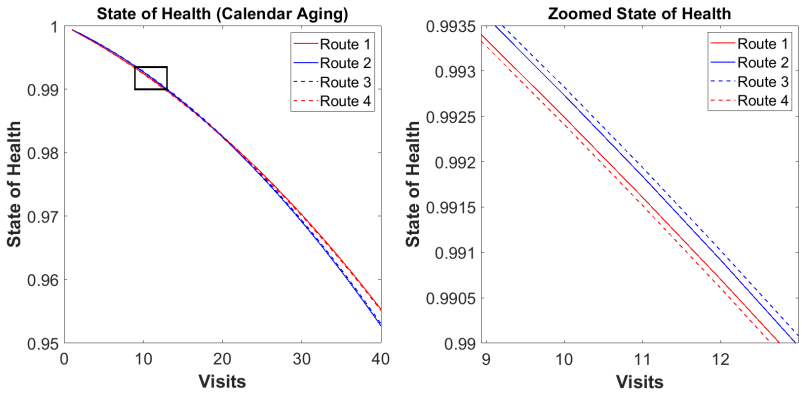

Figure 11: Comparison of state of health against visits when only considering calendar ageing.

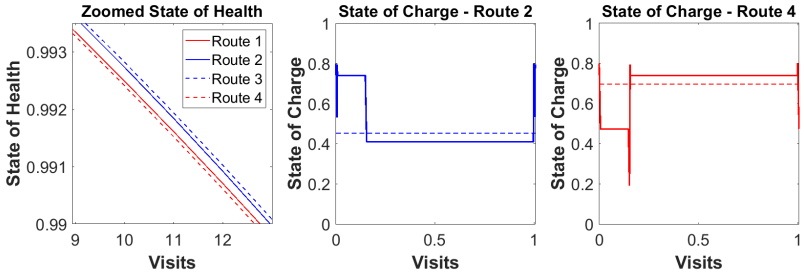

Figure 12: Comparison of state of health against visits when only considering calendar ageing for new batteries, with average state of charge highlighted for Routes 2 and 4.

We justify this behaviour via consideration of our calendar ageing function (equations (14) and (15)). We note that by construction, the functions $f(s)$ and $g(s)$ reach their minima at the optimal state of charge, but in general $g(s)$ is constructed to attain a minimum of 0 (meaning no further penalty incurred for storage at optimal state of charge), while $f(s)$ attains a minimum of 1 (the "base" degradation incurred when operating at $I \leq 1$ C). Thus, for "small" values of time t, we have

$$m_1 f(s) > m_2 g(s) t, \tag{28}$$

which implies that the long-term *storage* effects are more important than the penalty effects which are only active for the small periods when the vehicle is being driven (recalling that the $\frac{\partial Q}{\partial s}$ term is only active when the state of charge is changing).

Considering now old batteries, we note that eventually as $t \to \infty$ the inequality sign in (28) flips provided $s \neq 0.4$ - and so our penalty function is weighted higher when

considering degradation effects, that is to say we enter a situation in which

$$m_1 f(s) < m_2 g(s) t, \tag{29}$$

which is to say how we *use* an older battery is more important than how we *store* it. Bearing in mind that this penalty function is only in consideration when we drive and recalling the average state of charge values for driving profiles as shown in Figure 10, we observe that in fact the Routes 1 and 4 are *better* for using older batteries as they have an average state of charge much closer to the optimal value for ageing when driving - explaining why at late times Routes 2 and 3 incur greater battery degradation.

We thus present the total degradation over time in Figure 13 which demonstrates the results which we should now expect for usage recommendations, namely that:

1. For new batteries, storage at an optimal state of charge and usage near the optimal state of charge are both important concerns for minimising degradation.

2. For old batteries, penalty effects dominate and so any usage of the battery should be done as near to the optimal state of charge as possible, and storage effects are largely irrelevant.

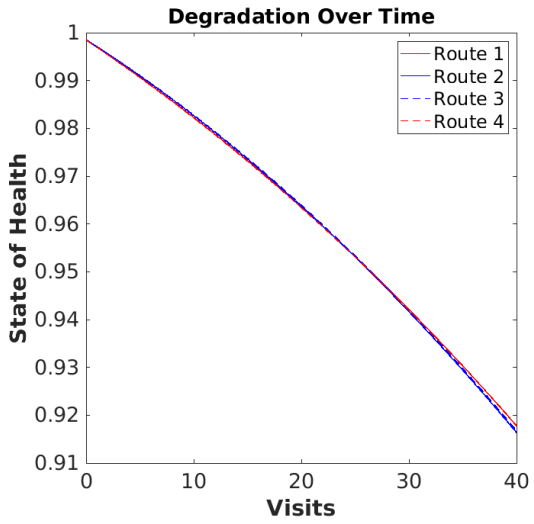

Figure 13: Comparison of state of health against visits with both cycle and calendar degradation.

5 Conclusions

Using a simple equivalent circuit model fitted to data on a specific battery, alongside a model for capacity degradation constructed using both information directly related to our battery and also batteries of similar chemistries, we have been able to construct a model to describe the evolution of the battery over time given some input usage profile. Further, we have explored this model in the context of a toy scenario pertaining to seeking the optimal usage profiles for an electric vehicle undergoing a weekly long-distance journey, and have explored how the differing effects within our model come into play within this scenario.

We have demonstrated that we may split the lifetime of a battery into two broad regimes, either "new" or "old", and have shown that both these regimes have different ideal usage profiles. Namely, storage effects are important for new batteries and so consideration of how batteries are kept long-term is of value, whereas for older batteries storage effects are dwarfed by the degradation effects incurred by usage of the battery at suboptimal states of charge.

However, there are some clear limitations of our model. Firstly, we have neglected any temperature based effects both in our ECM parameters and in the degradation model, when we know from observation of both the data sheet and HPPC curves that these effects do exist; the decision was made to exclude these effects in our analysis as some parameters (such as C_1 in the ECM) vary wildly with temperature and so in effect we would need to construct different models for different temperature ranges. Furthermore, as a result of not having exact data on how cycle degradation varies with current for *our* battery nor for how the shape of the optimal state of charge curves $g(s), f(s)$ look in our calendar ageing functions, we have been forced to make assumptions on how the capacity evolves over time - leading to us only to be able to give qualitative results for new and old batteries.

Some clear extensions for this project are thus to perform experimentation to observe how capacity degrades for different currents as a function of cycle count, and also to incorporate these temperature-based effects. With these tools in place, it should be straightforward to implement a more quantitative model as to be able to make recommendations for usage profiles for this battery, and indeed other batteries of similar chemistries.

6 References

[1] Hector Beltran, Pablo Ayuso, Nuria Vicente, Braulio Beltrán-Pitarch, Jorge García-Cañadas, and Emilio Pérez. "Equivalent circuit definition and calendar aging analysis of commercial Li(NixMnyCoz)O2/graphite pouch cells". In: *Journal of Energy Storage* 52 (Aug. 1, 2022), p. 104747. ISSN: 2352-152X. DOI: 10.1016/j.est.2022.104747. URL: https://www.sciencedirect.com/science/article/pii/S2352152X22007587 (visited on 03/09/2023).

[2] Matthieu Dubarry and Arnaud Devie. "Battery durability and reliability under electric utility grid operations: Representative usage aging and calendar aging". In: *Journal of Energy Storage* 18 (Aug. 1, 2018), pp. 185–195. ISSN: 2352-152X. DOI: 10.1016/j.est.2018.04.004. URL: https://www.sciencedirect.com/science/article/pii/S2352152X17306138 (visited on 03/09/2023).

[3] Ricardo Faria, Pedro Marques, Rita Garcia, Pedro Moura, Fausto Freire, Joaquim Delgado, and Aníbal T. de Almeida. "Primary and secondary use of electric mobility batteries from a life cycle perspective". In: *Journal of Power Sources* 262 (2014), p. 169. ISSN: 0378-7753. URL: https://www.academia.edu/28803334/Primary_and_secondary_use_of_electric_mobility_batteries_from_a_life_cycle_perspective (visited on 03/02/2023).

[4] Jakob Fleischmann, Mikael Hanicke, Evan Horetsky, Dina Ibrahim, Sören Jautelat, Martin Linder, Patrick Schaufuss, Lukas Torscht, and Alexandre van de Rijt. *Lithium-ion battery demand forecast for 2030 | McKinsey*. URL: https://www.mckinsey.com/industries/automotive-and-assembly/our-insights/battery-2030-resilient-sustainable-and-circular#/ (visited on 03/07/2023).

[5] Phillip Kollmeyer. "Panasonic 18650PF Li-ion Battery Data". In: 1 (June 21, 2018). Publisher: Mendeley Data. DOI: 10.17632/wykht8y7tg.1. URL: https://data.mendeley.com/datasets/wykht8y7tg/1 (visited on 03/02/2023).

[6] Emmanouil D. Kostopoulos, George C. Spyropoulos, and John K. Kaldellis. "Real-world study for the optimal charging of electric vehicles". In: *Energy Reports* 6 (Nov. 1, 2020), pp. 418–426. ISSN: 2352-4847. DOI: 10.1016/j.egyr.2019.12.008. URL: https://www.sciencedirect.com/science/article/pii/S2352484719310911 (visited on 04/11/2023).

[7] Mathworks. *ode15s - MATLAB Documentation*. URL: https://uk.mathworks.com/help/matlab/ref/ode15s.html (visited on 04/11/2023).

[8] *NCR18650PF | Panasonic Industrial Devices*. URL: https://na.industrial.panasonic.com/products/batteries/rechargeable-batteries/lineup/lithium-ion/series/90729/model/90730 (visited on 03/02/2023).

[9] Naoki Nitta, Feixiang Wu, Jung Tae Lee, and Gleb Yushin. "Li-ion battery materials: present and future". In: *Materials Today* 18.5 (June 1, 2015), pp. 252–264. ISSN: 1369-7021. DOI: 10.1016/j.mattod.2014.10.040. URL: https://www.sciencedirect.com/science/article/pii/S1369702114004118 (visited on 04/09/2023).

[10] *Panasonic - Lithium Ion Batteries Technical Handbook*. URL: https://eu.industrial.panasonic.com/sites/default/pidseu/files/downloads/files/panasonic_li-ion_handbook.pdf (visited on 04/10/2023).

[11] *Panasonic NCR 18650PF Cell 3.7 V - 2900 mAh [NMC-0370029-18650P]*. URL: https://www.liontecshop.com/shop/18650-26650-nmc-and-lfp/panasonic-ncr-18650pf-cell-3-7-v-2900-mah-p-234 (visited on 03/02/2023).

[12] Aramis Perez, Vanessa Quintero, Francisco Jaramillo Montoya, Heraldo Rozas, Diego Jimenez, Marcos Orchard, and Rodrigo Moreno. "Characterization of the degradation process of lithium-ion batteries when discharged at different current rates". In: *Proceedings of the Institution of Mechanical Engineers Part I Journal of Systems and Control Engineering* 232 (Aug. 1, 2018), pp. 1075–1089. DOI: 10.1177/0959651818774481.

[13] Gregory L. Plett. *Battery management systems, Volume I: Battery modeling*. Vol. 1. Artech House, 2015.

[14] Simon F. Schuster, Tobias Bach, Elena Fleder, Jana Müller, Martin Brand, Gerhard Sextl, and Andreas Jossen. "Nonlinear aging characteristics of lithium-ion cells under different operational conditions". In: *Journal of Energy Storage* 1 (June 1, 2015), pp. 44–53. ISSN: 2352-152X. DOI: 10.1016/j.est.2015.05.003. URL: https://www.sciencedirect.com/science/article/pii/S2352152X15000092 (visited on 04/10/2023).

[15] Adrian Soto, Alberto Berrueta, Miren Mateos, Pablo Sanchis, and Alfredo Ursúa. "Impact of micro-cycles on the lifetime of lithium-ion batteries: An experimental study". In: *Journal of Energy Storage* 55 (Nov. 1, 2022), p. 105343. ISSN: 2352-152X. DOI: 10.1016/j.est.2022.105343. URL: https://www.sciencedirect.com/science/article/pii/S2352152X2201338X (visited on 03/02/2023).

[16] Daniel Werner, Sabine Paarmann, and Thomas Wetzel. “Calendar Aging of Li-Ion Cells—Experimental Investigation and Empirical Correlation”. In: *Batteries* 7.2 (June 2021). Number: 2 Publisher: Multidisciplinary Digital Publishing Institute, p. 28. ISSN: 2313-0105. DOI: 10.3390/batteries7020028. URL: https://www.mdpi.com/2313-0105/7/2/28 (visited on 03/09/2023).

Appendices

A Polynomial Fits for ECM Parameters

$$
\begin{aligned}
R_0(s) &= 0.99s^6 - 2.26s^5 + 1.93s^4 - 0.93s^3 + 0.52s^2 - 0.52s - 0.25,\\
R_1(s) &= 24.94s^6 - 89.93s^5 + 130.05s^4 - 96.3s^3 + 38.45s^2 - 7.8s + 0.65,\\
C_1(s) &= -839.66 \times 10^3 s^4 + 2.12 \times 10^6 s^3 - 2.06 \times 10^6 s^2 + 906.76 \times 10^3 s - 101 \times 10^3,\\
V_{OC}(s) &= 10.60s^5 - 33.52s^4 + 40.17s^3 - 22.18s^2 + 6.28s + 2.81
\end{aligned}
$$

B Capacity Degradation Function

$$
\begin{aligned}
Q(t,c,s,I) = Q_0 &- \frac{c\left(1.32 \times 10^{-3} + 2.9\exp\left\{5.07 \times 10^{-2}c - 35.49\right\}\right)}{1.02 - \exp\{0.30I - 5.07\}}\\
&- \int_0^t dt\left(9.20 \times 10^{-10}\cosh(0.4s - 0.16) + 3.67 \times 10^{-10}t\left|\sinh(0.4s - 0.16)\right|\left|\frac{ds}{dt}\right|\right)
\end{aligned}
$$